American Mineralogist, Volume 75, pages 141–149, 1990

Difference displacement parameters in alkali feldspars: Effects of (Si,Al) order-disorder

MARTIN KUNZ, THOMAS ARMBRUSTER
Laboratory for Chemical and Mineralogical Crystallography, University of Bern, Freiestrasse 3, CH-3012 Bern, Switzerland

ABSTRACT

Anisotropic mean-square displacement parameters, as routinely obtained from single-crystal structure refinements, are used to calculate difference values (ΔU) along the (Si,Al)-O vector in alkali feldspar tetrahedra. ΔU values averaged over a tetrahedron ($\langle \Delta U \rangle$) provide physical information on (Si,Al) order-disorder.

In the framework tetrahedra of feldspars, mean (Si,Al)-O bond lengths range from 1.61 Å to 1.74 Å, mainly depending on the (Si,Al) population of symmetrically equivalent tetrahedral sites. Values of $\langle \Delta U \rangle$ calculated for 153 individual tetrahedra in a sample of 49 (Si,Al)-ordered and (Si,Al)-disordered structures vary as a quadratic function of the mean (Si,Al)-O distance. This correlation may be understood in terms of a distribution of disordered oxygen atoms over two positions that are 0.13 Å apart, leading to an increase of difference displacement parameters ($\langle \Delta U \rangle$) with increasing (Si,Al) disorder. $\langle \Delta U \rangle$ for a SiO_4 tetrahedron is 0.0004 Å^2 and 0.0005 Å^2 for an AlO_4 tetrahedron, whereas a tetrahedron with 50% Al and 50% Si yields $\langle \Delta U \rangle \approx 0.004$ Å^2.

Difference displacement parameters in feldspars are sensitive to (1) (Si,Al) order-disorder, (2) errors in the model of a structure refinement, and (3) errors in lists of anisotropic displacement parameters.

INTRODUCTION

Anisotropic displacement parameters are routinely published for many crystal structures refined from X-ray or neutron diffraction experiments. However, these parameters are only rarely used to extract physical information. Differences between anisotropic mean-square displacement parameters evaluated along internuclear directions (difference displacement parameters or ΔU values) have been shown to provide information on static and dynamic disorder in crystals (Bürgi, 1984), especially if the ΔU values are averaged ($\langle \Delta U \rangle$) over a coordination polyhedron. The results of a study on the high-spin–low-spin transition in crystalline *tris*(dithiocarbamato)iron(III) complexes (Chandrasekhar and Bürgi, 1984) indicated that (1) $\langle \Delta U \rangle$ values determined experimentally are quite reliable and tend to be less affected by systematic errors than the U values themselves, because systematic errors in U tend to cancel on taking the difference. (2) $\langle \Delta U \rangle$ values might provide information on (Si,Al) disorder in Al-substituted silicates. With these findings as a background, difference displacement parameters in feldspars have been studied. Typical values of $\langle \Delta U \rangle$ for Si-O and Al-O bonds in alkali feldspars are given, and the dependence of $\langle \Delta U \rangle$ on the degree of (Si,Al) disorder in alkali feldspars in general is discussed. In an accompanying paper (Armbruster et al., 1990), the effect of experimental parameters on isotropic displacement parameters (B_{eq} values) has been investigated for low albite.

(Si,Al) order-disorder in alkali feldspars

In feldspars, mean Al-O distances are ~1.74 Å and mean Si-O distances are ~1.61 Å. (Si,Al)-O distances determined by X-ray or neutron diffraction experiments yield a space- and time-averaged value over all symmetrically equivalent sites. Thus, the observed (Si,Al)-O distance is mainly a function of the (Si,Al) distribution among the tetrahedral sites of the framework (Jones, 1968; Ribbe and Gibbs, 1969; Ribbe, 1983). In a similar manner, it can be expected that in a disordered structural state, anisotropic displacement parameters refined from diffraction experiments reflect the difference between Si-O and Al-O bonds. This relation between anisotropic displacement parameters and (Si,Al)-O distances has been verified by examination of sets of feldspar structure refinements retrieved from the literature.

The tetrahedral framework of ideal alkali feldspars, $(Na,K)AlSi_3O_8$, contains SiO_4 and AlO_4 tetrahedra in a ratio of 3/1. In a perfectly ordered state (space $C\bar{1}$), Al occupies the T_1O site, while Si atoms are found in the remaining tetrahedral sites (T_1m, T_2O, T_2m). For such a crystal the occupancy [Al/(Al + Si)] is $t_1o = 1.0$, and $t_1m = t_2o = t_2m = 0.0$ (Kroll, 1971). In a hypothetical, totally

0003–004X/90/0102–0141$02.00

TABLE 1. Experimental conditions and refinement models for alkali feldspar structures

Ref.*	Feldspar	Sample no. or source	Composition				Temperature	No. of reflections	sin θ/λ	Correction	
			Or	Ab	An	Cn				Abs.	Ext.
1a	Monalbite	Amelia	0.006	0.993	0.001		1253 K	1054	<0.7	n.s.	n.s.
2	Ba-feldspar		0.59	0.22		0.19	RT	1346	<0.756	yes	n.s.
3a	Sanidine		0.65	0.35			RT	924	<0.7	yes	n.s.
4a	*Sanidine*	*SAGT*	*0.85*	*0.14*		*0.01*	*RT***	*3450*	*<1.19*	*no*	*yes*
4b	*Sanidine*	*SVG1*	*0.85*	*0.14*		*0.01*	*RT*	*5703*	*<1.2*	*no*	*yes*
4c	Sanidine	SATO	0.85	0.14		0.01	RT**	12204	<1.0	yes	yes
4d	Sanidine	SANI	0.85	0.14		0.01	RT**	6378	<1.08	yes	yes
4e	Sanidine	SAAT	0.85	0.14		0.01	RT**	8617	<1.10	yes	yes
4f	Sanidine	STOT	0.85	0.14		0.01	RT**	9816	<1.10	yes	yes
4g	Sanidine	SAGA	0.85	0.14		0.01	RT	17226	<1.19	yes	yes
4h	*Sanidine*	*SANG*	*0.85*	*0.14*		*0.01*	*RT***	*2774*	*<0.99*	*no*	*yes*
4i	*Sanidine*	*SVG3*	*0.85*	*0.14*		*0.01*	*RT***	*2137*	*<0.74*	*no*	*yes*
4j	Sanidine	SAND	0.85	0.14		0.01	RT**	6990	<1.08	yes	yes
4k	*Sanidine*	*SANU*	*0.85*	*0.14*		*0.01*	*RT***	*2075*	*<0.94*	*no*	*yes*
4l	Sanidine	SANN	0.85	0.14		0.01	RT**	9319	<1.08	yes	yes
5a	Sanidine		0.854	0.145	0.001		RT	1074	<0.6	no	no
6a	Sanidine		0.87	0.13			RT**	2000	<0.95	no	n.s.
6b	Sanidine		0.87	0.13			RT	2000	<0.95	no	n.s.
5b	Adularia		0.879	0.119	0.002		RT	1114	<0.6	no	no
4m	Orthoclase		0.931	0.069			RT	11456	<1.23	yes	yes
7	Sanidine	Upper mantle	0.976	0.018	0.002	0.004	RT	2150	<1.27	yes	n.s.
1b	High albite		0.0025	0.9975			298 K	2443	<0.75	n.s.	n.s.
8	*Low albite*	*Amelia*	*0.006*	*0.993*	*0.001*		*13 K*	*2662*	*<0.784*	*yes*	*yes*
9a	*Low albite*	*Amelia*	*0.006*	*0.993*	*0.001*		*RT*	*1633*	*<0.69*	*yes*	*n.s.*
9b	Low albite	Amelia	0.006	0.993	0.001		RT	2441	<0.76	yes	yes
10a	Low albite	Tiburon	0.0025	0.9975			773 K	1980	n.s.	yes	no
10b	Low albite	Tiburon	0.0025	0.9975			1023 K	1990	n.s.	yes	no
10c	Low albite	Tiburon	0.0025	0.9975			1243 K	2002	n.s.	yes	no
11	Low albite	Roc Tourné	0.001	0.999			RT	3370	<0.9	no	yes
12a	Low albite	Ramona	0.001	0.985	0.005		RT	1994††	n.s.	no	no
12b	High albite		0.016	0.977	0.007		RT	1797††	n.s.	n.s.	n.s.
13a	Anorthoclase	Kaknui	0.121	0.840	0.039		RT	2141	<0.705	no	no
3b	High albite		0.22	0.78			296 K	1698	<0.85	yes	n.s.
13b	Anorthoclase	Mt. Gibele	0.223	0.708	0.069		RT	1697	<0.705	no	no
13c	Anorthoclase	Gr. Caldeira	0.325	0.667	0.008		RT	1834	<0.705	no	no
14	Microcline		0.80	0.19	0.01		RT	1207	<0.7035	yes	n.s.
15	Microcline	Spencer U	0.846	0.125	0.014		RT	2124††	n.s.	n.s.	n.s.
16a	K-feldspar	RC20C	0.855	0.133	0.009	0.003	RT	1773	<0.7	no	n.s.
16b	K-feldspar	P17C	0.871	0.120	0.001	0.000	RT	1738	<0.7	no	n.s.
16c	K-feldspar	CA1A	0.886	0.099	0.003	0.012	RT	1640	<0.7	no	n.s.
16d	K-feldspar	CA1B	0.886	0.099	0.003	0.012	RT	1637	<0.7	no	n.s.
16e	K-feldspar	CA1E	0.886	0.099	0.003	0.012	RT	1737	<0.7	no	n.s.
16f	K-feldspar	P1C	0.900	0.088	0.005	0.007	RT	1455	<0.7	no	n.s.
16g	K-feldspar	A1D	0.904	0.085	0.005	0.006	RT	1907	<0.7	no	n.s.
17	Microcline‡		0.91	0.06		0.03	RT	893	<0.6	no	n.s.
16h	K-feldspar	P2A	0.931	0.055	0.009	0.005	RT	1587	<0.7	no	n.s.
16i	K-feldspar	P2B	0.931	0.055	0.009	0.003	RT	1638	<0.7	no	n.s.
18a	Microcline	7813A	0.943	0.052		0.001	RT	1236	<0.68	yes	n.s.
18b	Microcline	7813B	0.943	0.052		0.001	RT	1201	<0.68	yes	n.s.

Note: Entries written in italics refer to neutron data; Or = orthoclase ($KAlSi_3O_8$), Ab = albite ($NaAlSi_3O_8$), An = anorthite ($CaAl_2Si_2O_8$), Cn = celsian ($BaAl_2Si_2O_8$). RT = room temperature; n.s. = not specified; abs. = correction for absorption; ext. = correction for extinction; anom. disp. = correction for anomalous dispersion (f', f''); R = residual factor; R_w = weighted residual factor.

* References: (1) Winter et al. (1979), (2) Viswanathan and Kielhorn (1983), (3) Keefer and Brown (1978), (4) Gering (1985), (5) Phillips and Ribbe (1973), (6) Weitz (1972), (7) Scambos et al. (1987), (8) Smith et al. (1986), (9) Harlow and Brown (1980), (10) Winter et al. (1977), (11) Armbruster et al. (1990), (12) Ribbe et al. (1969), (13) Harlow (1982), (14) Blasi et al. (1981), (15) Bailey (1969), (16) Dal Negro et al. (1978), (17) Ribbe (1979), (18) Blasi et al. (1984).

** Annealing conditions before the experiment: SAGT—1323 K, 500 h. SATO—1023 K, 1500 h. SANI—1223 K, 20 h. SAAT—1323 K, 0.25 h. STOT—923 K, 2000 h. SANG—1123 K, 1200 h. SVG3—1223 K, 20 h. SAND—1323 K, 500 h. SANU—1123 K, 1200 h. SANN—1323 K, 500 h. Sanidine from reference 6a—1023 K.

† N = neutral atom. I = ionic.

†† Film.

‡ Cryptoperthitic.

disordered specimen (space group $C2/m$), Al/(Al + Si) is equal for all positions ($t_1o = t_1m = t_2o = t_2m = 0.25$).

EXPERIMENTAL PROCEDURE

Data retrieval

Originally, 62 feldspar structure refinements reported with anisotropic displacement parameters (β_{ij} or U_{ij}) were retrieved from the literature. This random selection is not complete but was considered sufficient to study the influence of (Si,Al) order-disorder on $\langle \Delta U \rangle$. No restrictions were made concerning experimental and refinement procedures. During data organization, it became obvious that plagioclases ($(Na_xCa_{1-x})[Al_{2-x}Si_{2+x}O_8]$), if compared to alkali feldspars, show different ordering mechanisms and submicroscopic exsolution and intergrowth structures.

TABLE 1.—*Continued*

Scattering factor†	Weighting	Anom. disp.	R (%)	R_w (%)	Space group
N	$1/\sigma^2$	yes	4.9	3.9	$C2/m$
N	n.s.	yes	4.2	n.s.	$C2/m$
N	$1/\sigma^2$	n.s.	2.9	3.3	$C2/m$
(neutrons)	*n.s.*	*n.s.*	*2.7*	*1.5*	$C2/m$
(neutrons)	*n.s.*	*n.s.*	*3.6*	*3.2*	$C2/m$
N + I	n.s.	n.s.	2.9	3.0	$C2/m$
N + I	n.s.	n.s.	2.5	2.6	$C2/m$
N + I	n.s.	n.s.	2.2	2.5	$C2/m$
N + I	n.s.	n.s.	2.5	2.5	$C2/m$
N + I	n.s.	n.s.	2.7	3.1	$C2/m$
(neutrons)	*n.s.*	*n.s.*	*2.2*	*2.2*	$C2/m$
(neutrons)	*n.s.*	*n.s.*	*1.6*	*1.5*	$C2/m$
N + I	n.s.	n.s.	2.3	3.0	$C2/m$
(neutrons)	*n.s.*	*n.s.*	*2.5*	*1.9*	$C2/m$
N + I	n.s.	n.s.	2.5	2.7	$C2/m$
N	n.s.	n.s.	3.8	4.7	$C2/m$
n.s.	n.s.	n.s.	8.3	n.s.	$C2/m$
n.s.	n.s.	n.s.	8.5	n.s.	$C2/m$
N	n.s.	n.s.	4.3	4.6	$C2/m$
N + I	n.s.	n.s.	3.7	3.0	$C2/m$
n.s.	n.s.	n.s.	5.5	4.7	$C2/m$
N	$1/\sigma^2$	yes	3.4	4.0	$C\bar{1}$
(neutrons)	*n.s.*	*n.s.*	*2.2*	*3.0*	$C\bar{1}$
(neutrons)	*n.s.*	*n.s.*	*2.1*	*2.4*	$C\bar{1}$
N + I	n.s.	n.s.	4.0	3.5	$C\bar{1}$
N	n.s.	n.s.	3.2	n.s.	$C\bar{1}$
N	$1/\sigma^2$	n.s.	3.5	n.s.	$C\bar{1}$
N	$1/\sigma^2$	n.s.	3.9	n.s.	$C\bar{1}$
N	$1/\sigma^2$	yes	2.0	3.4	$C\bar{1}$
½ I	n.s.	n.s.	6.8	n.s.	$C\bar{1}$
½ I	n.s.	n.s.	8.2	n.s.	$C\bar{1}$
N	$1/\sigma$	n.s.	5.8	5.2	$C\bar{1}$
N	$1/\sigma^2$	n.s.	8.3	9.6	$C\bar{1}$
N	$1/\sigma$	n.s.	4.7	4.1	$C\bar{1}$
N	$1/\sigma$	n.s.	4.6	4.6	$C\bar{1}$
N	$1/\sigma^2$	yes	4.7	4.9	$C\bar{1}$
½ I	1	n.s.	8.0	n.s.	$C\bar{1}$
N	n.s.	n.s.	3.5	n.s.	$C\bar{1}$
N	n.s.	n.s.	3.2	n.s.	$C\bar{1}$
N	n.s.	n.s.	3.6	n.s.	$C\bar{1}$
N	n.s.	n.s.	3.8	n.s.	$C\bar{1}$
N	n.s.	n.s.	2.8	n.s.	$C\bar{1}$
N	n.s.	n.s.	5.3	n.s.	$C\bar{1}$
N	n.s.	n.s.	2.4	n.s.	$C\bar{1}$
n.s.	n.s.	n.s.	4.9	n.s.	$C\bar{1}$
N	n.s.	n.s.	3.4	n.s.	$C\bar{1}$
N	n.s.	n.s.	3.5	n.s.	$C\bar{1}$
n.s.	$1/\sigma^2$	n.s.	3.3	3.3	$C\bar{1}$
n.s.	$1/\sigma^2$	n.s.	3.1	3.4	$C\bar{1}$

Consequently, data of feldspars with components of anorthite ($CaAl_2Si_2O_8$) and/or celsian ($BaAl_2Si_2O_8$) > 30% were rejected. The final alkali feldspar data set contains 49 structures (28 in space group $C\bar{1}$ and 21 in space group $C2/m$) with 154 individual tetrahedra (Table 1). Most structures were determined at room temperature (RT) with the exceptions of the Amelia monalbite (1253 K) of Winter et al. (1979), the low albite (neutron data, 13 K) of Smith et al. (1986), and the low albite (773 K, 1023 K, 1243 K) of Winter et al. (1977). Seven intensity data sets were collected with neutrons and 42 with Mo$K\alpha$ X-radiation. Intensity data for three structures were recorded on films.

Conventional unweighted R values vary between 1.6% and 8.5%. As noticed by Chandrasekhar and Bürgi (1984), authors are often not very careful in reporting their experimental details. In many cases it remains dubious (1) what kind of scattering factors were used (e.g., neutral or ionized), (2) whether anomalous dispersion corrections (f' and f'') were applied, (3) whether absorption or extinction corrections were applied, (4) which reflections were used for structure refinement (cutoff, sin θ/λ limit), or (5) which kind of weighting scheme was used for data refinement. Such missing or not explicitly stated "details" are marked "n.s." (not specified) in Table 1.

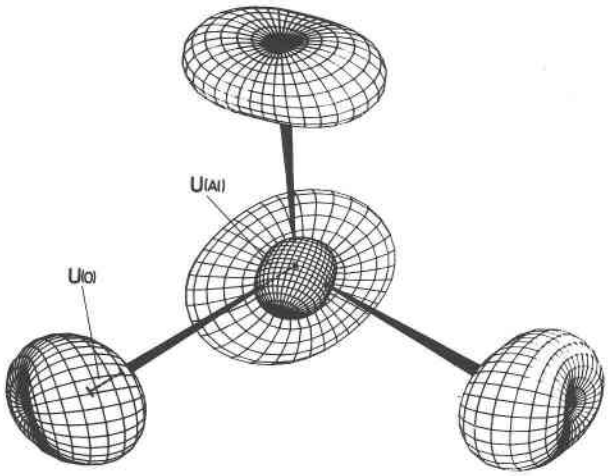

Fig. 1. Arbitrarily oriented AlO_4 tetrahedron displaying mean-square displacement ovaloids for oxygen atoms and Al of low albite at 1243 K (data from Winter et al., 1977). U(O) and U(Al) are marked for one selected vector (graphic program by W. Hummel).

Data processing

The program THMV9 (Trueblood, personal communication) was used to calculate (Si,Al)-O bond distances, individual mean-square displacements, U_i along the (Si,Al)-O vector as well as the differences $\Delta U = (U_{(O)} - U_{(Si,Al)})$ in these directions and rotation tensors from anisotropic displacement parameters. A precursor version of this program has been discussed by Schomaker and Trueblood (1968) and Trueblood (1978).

It must be noted at this point that the representational surface of anisotropic mean-square displacement parameters U_{ij} may lead to "peanut-shaped" ovaloids (Nelmes, 1969) and not to ideal ellipsoids as one might assume at first glance. Figure 1 displays mean-square displacement surfaces at 1243 K for a low albite T_1O(Al) tetrahedron [data from Winter et al. (1977)]. In contrast, ellipsoids as displayed by the program ORTEP by Johnson (1976) represent probability ellipsoids of atomic displacements.

Individual ΔU values within one tetrahedron may differ in magnitude and sign, depending on whether the extension of the (Si,Al)-O distance due to Al → Si substitution is absorbed primarily by the oxygen or the (Si,Al) position. Figure 2 shows two extreme cases where (a) the T atom position and (b) the oxygen position remains unchanged. As shown in Appendix 1, averaging over all four ΔU values in a tetrahedron removes this ambiguity and the effects related to rigid-body translation (Chandrasek-

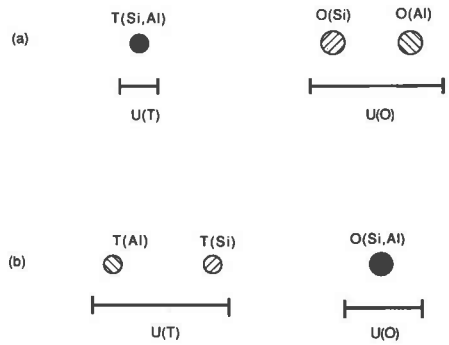

Fig. 2. Effect of displacement caused by Al → Si substitution on a difference displacement parameter $\Delta U = U(O) - U(T)$. **(a)** The extension acts on the oxygen atom only, and ΔU will be positive. **(b)** The case where only the T atom is displaced, causing ΔU to become negative. There are various mixed states between these two extremes.

har and Bürgi, 1984). Thus the origin of the reference system is placed on the (Si,Al) site. For each tetrahedron, an average (Si,Al)-O distance (⟨T-O⟩) and average ΔU (⟨ΔU⟩) values were calculated (Table 2).

Rigid-body libration due to temperature and Al → Si substitution

The effect of temperature is analyzed for low albite for which data are available between 13 and 1243 K (Smith et al., 1986; Winter et al., 1977). Equivalent isotropic displacement parameters (B_{eq} values) for (Si,Al) increase from 0.2 at 13 K to 2.0 Å² at 1243 K, while corresponding values for oxygen increase from 0.4 to 4.0 Å². The increase in B_{eq}(oxygen) and B_{eq}(Si,Al) with temperature has no significant effect on ⟨ΔU⟩ values, which remain constant to within 1–2 ⟨$\sigma(\Delta U)$⟩ over the entire temperature range (Table 2). The results imply increased rigid-body translational and oscillational motion of the TO_4 fragment as temperature increases, but only a very slight increase in the T-O stretching motion. Analysis of rigid-body libration of individual tetrahedral units between 13 K and 1243 K indicates that T-O distances at 1243 K should be increased by ca. 0.015 Å to compensate for apparent bond shortening due to the use of Gaussian anisotropic displacement parameters (Schomaker and Trueblood, 1968). Since the observed T-O distances are found to be essentially constant throughout the whole temperature range, the apparent shortening due to libration seems to be compensated by a lengthening due to anharmonicity in the T-O stretching motion (Kuchitsu and Bartell, 1961). This effect is estimated to be ca. 0.01 Å.

The influence of Al → Si substitution on rigid-body rotation of a TO_4 fragment was analyzed on the basis of rotation tensors for each tetrahedron of a microcline [well-ordered K-feldspar (Dal Negro et al., 1978)] and a sanidine [disordered K-feldspar (Scambos et al., 1987)]. Comparison of corresponding rotation tensors reveals that the effect of Al → Si substitution lies within a few esd's of the tensor components for both T_1 and T_2 tetrahedra.

Tetrahedral distortion due to Al → Si substitution

A principal-component analysis (Chatfield and Collins, 1980), on 10 independent parameters (four T-O and six O-O distances) was carried out separately for T_1 and T_2 tetrahedra in order to analyze the influence of an individual T-O bond on the remaining distances within a tetrahedron. Distances were represented as deviations from their respective means, expressed in units of corresponding standard deviations. The bivariate statistics for T_1 and T_2 tetrahedra yield one distinct factor, whose eigenvalue is much higher than the other ones (96% and 67% of the total correlation, respectively). The correlation is considerably poorer for T_2 than for T_1 tetrahedra because in well-ordered alkali feldspar, Al concentrates on T_1O. Only minor Al concentrations are found on T_2, which leads to a limited data set for statistical treatment. With the eigenvectors of the highest factors, the mutual influence of individual T-O and O-O distances can be determined from one single distance as shown in Appendix 2. One characteristic Si-O distance and one Al-O distance coupled with trigonometric calculations (also expanded in App. 2) lead to prototype SiO_4 and AlO_4 tetrahedra representing distances and inclination angles to be expected for an Al → Si substitution (App. 2). It is evident from these calculations that owing to Al → Si substitution, displacement vectors of oxygen atoms are inclined by only few degrees to the T-O bonding vector. The amount of this inclination (ϵ) seems to be rather small (ϵ up to 2.6° for T_1 tetrahedra and 6.8° for T_2 tetrahedra). A hypothetical inclination of $\epsilon = 10°$ decreases the apparent difference $d_{(Al\text{-}O)} - d_{(Si\text{-}O)}$ along the T-O vector by some 10^{-4} Å. Most interatomic distances in feldspars are accurate within 10^{-2} to 10^{-3} Å. Thus the effect of inclination is within the accuracy limits of T-O distances, and a corresponding correction can be neglected.

Results

⟨ΔU⟩ values for SiO_4 and AlO_4 tetrahedra

The highest degree of (Si,Al) ordering within our data set is observed for various low albites. Thus, this phase is the most suitable to characterize SiO_4 and AlO_4 end-members. In addition, the quality of low albite displacement parameters has been critically discussed in an accompanying paper (Armbruster et al., 1990). Room-temperature data of Harlow and Brown (1980) and Armbruster et al. (1990), 13-K data of Smith et al. (1986), and high-temperature data (773 K, 1023 K, 1243 K) of Winter et al. (1977) were applied. For the Al tetrahedron, T_1O, an average ⟨ΔU⟩ value of 0.0005 Å² (weighted $1/\sigma^2$) was calculated. For the Si tetrahedra, T_1m, T_2O, and T_2m, corresponding averages are 0.0004, 0.0005, and 0.0004 Å², respectively. These values serve as a reference to gauge the effect of (Si,Al) disorder.

TABLE 2. Mean distances $\langle d \rangle$ (Å) and mean difference displacement parameters × 10^4 $\langle \Delta U \rangle$ (Å²) along the T-O direction for alkali feldspar structures

T_1O		T_1m		T_2O		T_2m		
$\langle d \rangle$	$\langle \Delta U \rangle$	$\langle d \rangle$	$\langle \Delta U \rangle$	$\langle d \rangle$	$\langle \Delta U \rangle$	$\langle d \rangle$	$\langle \Delta U \rangle$	Ref.
1.647(3)	39(14)			1.636(3)	43(14)			1a
1.668(2)	71(11)			1.638(2)	46(11)			2
1.651(1)	47(9)			1.638(1)	44(8)			3a
1.6454(5)	43(1)			1.6401(6)	38(2)			4a
1.6505(7)	47(2)			1.6353(7)	35(2)			4b
1.6487(10)	43(5)			1.6367(10)	34(5)			4c
1.6443(9)	41(4)			1.6402(10)	40(4)			4d
1.6463(7)	41(3)			1.6378(7)	35(3)			4e
1.6498(8)	44(4)			1.6350(8)	36(3)			4f
1.6500(8)	36(3)			1.6348(8)	35(3)			4g
1.6473(6)	45(2)			1.6390(7)	40(2)			4h
1.6508(6)	41(2)			1.6355(6)	39(2)			4i
1.6468(8)	40(3)			1.6385(8)	36(3)			4j
1.6508(7)	39(2)			1.6351(7)	34(2)			4k
1.6445(8)	38(3)			1.6400(8)	39(3)			4l
1.649(3)	66(11)			1.637(3)	60(10)			5a
1.645(2)	124(15)			1.641(2)	116(21)			6a
1.653(2)	132(17)			1.635(2)	117(13)			6b
1.665(3)	61(12)			1.621(3)	47(11)			5b
1.6645(6)	49(2)			1.6210(6)	22(2)			4m
1.644(1)	57(8)			1.639(1)	53(8)			7
1.649(2)	43(10)	1.642(2)	34(10)	1.641(2)	38(10)	1.643(2)	41(10)	1b
1.7438(5)	6(3)	1.6108(5)	3(2)	1.6148(4)	4(2)	1.6165(5)	3(2)	8
1.743(1)	0(4)	1.6087(8)	6(3)	1.6141(8)	6(3)	1.6156(8)	4(3)	9a
1.742(2)	7(10)	1.607(2)	21(10)	1.615(2)	20(10)	1.616(2)	25(10)	9b
1.741(2)	13(11)	1.607(2)	14(11)	1.613(2)	14(9)	1.615(2)	13(11)	10a
1.740(2)	14(11)	1.607(2)	14(11)	1.613(2)	15(11)	1.614(2)	13(11)	10b
1.740(2)	15(12)	1.605(2)	17(12)	1.610(2)	11(11)	1.613(2)	26(13)	10c
1.741(2)	4(3)	1.609(2)	3(3)	1.614(2)	4(3)	1.616(2)	3(3)	11
1.747(4)	−3(20)	1.611(4)	46(20)	1.616(4)	34(20)	1.614(5)	27(20)	12a
1.646(5)	65(20)	1.643(5)	55(20)	1.638(5)	107(20)	1.642(5)	53(20)	12b
1.649(3)	47(15)	1.645(3)	68(15)	1.639(3)	58(15)	1.641(3)	48(15)	13a
1.657(5)	42(18)	1.657(5)	43(17)	1.638(4)	21(18)	1.643(1)	60(19)	3b
1.648(3)	66(18)	1.645(3)	62(18)	1.639(3)	62(16)	1.643(3)	57(16)	13b
1.650(3)	48(14)	1.647(3)	54(14)	1.635(3)	61(14)	1.636(3)	60(14)	13c
1.677(4)	63(18)	1.660(4)	59(18)	1.620(4)	24(18)	1.619(4)	38(18)	14
1.695(5)	56(16)	1.641(5)	58(15)	1.620(5)	44(17)	1.616(5)	28(17)	15
1.717(2)	38(10)	1.630(2)	36(11)	1.616(2)	18(9)	1.616(2)	15(11)	16a
1.668(2)	56(10)	1.653(2)	57(10)	1.622(2)	31(9)	1.620(2)	26(9)	16b
1.674(2)	53(11)	1.661(2)	56(12)	1.625(2)	34(13)	1.624(2)	22(13)	16c
1.694(2)	59(12)	1.642(2)	44(12)	1.618(2)	25(13)	1.618(2)	23(12)	16d
1.733(2)	26(8)	1.620(2)	17(8)	1.618(2)	18(8)	1.618(2)	17(8)	16e
1.700(4)	42(18)	1.629(4)	23(18)	1.619(4)	20(18)	1.618(4)	16(18)	16f
1.673(2)	40(17)	1.650(2)	54(7)	1.623(2)	24(7)	1.621(2)	29(7)	16g
1.671(5)	117(30)	1.653(5)	120(30)	1.623(5)	85(30)	1.626(5)	77(29)	17
1.663(2)	49(10)	1.654(2)	49(10)	1.624(2)	35(10)	1.625(2)	34(10)	16h
1.659(2)	49(11)	1.656(2)	53(11)	1.630(2)	34(12)	1.629(2)	35(11)	16i
1.738(3)	12(15)	1.615(3)	14(14)	1.613(3)	10(14)	1.614(3)	9(15)	18a
1.738(3)	13(15)	1.612(3)	3(15)	1.615(3)	5(15)	1.613(3)	3(14)	18b

Note: For references, see Table 1; mean esd's of distances, $\langle \sigma(d) \rangle$, and mean esd's of ΔU values, $\langle \sigma(\Delta U) \rangle$, in parentheses.

Effect of (Si,Al) disorder on $\langle \Delta U \rangle$

As suggested by Chandrasekhar and Bürgi (1984), the effect of (Si,Al) disorder can be modeled as follows:

$$\langle \Delta U \rangle = p[\langle \Delta U_{(Si)} \rangle + \Delta^2_{(Si)}] + (1 - p)[\langle \Delta U_{(Al)} \rangle + \Delta^2_{(Al)}], \quad (1)$$

where $\Delta_{(Si)} = d_{obs} - d(\text{Si-O})$, $\Delta_{(Al)} = d(\text{Al-O}) - d_{obs}$, $\langle \Delta U_{(Si)} \rangle = 0.0004$ Å², $\langle \Delta U_{(Al)} \rangle = 0.0005$ Å², and $d_{obs} = \langle \text{T-O} \rangle$. The population factor p is defined by the formula

$$p = (d_{obs} - d(\text{Al-O})/(d(\text{Si-O}) - d(\text{Al-O})) = (d_{obs} - 1.74)/(-0.13), \quad (2)$$

where $d(\text{Si-O}) = 1.61$ Å and $d(\text{Al-O}) = 1.74$ Å. Substituting Equation 2 in Equation 1 yields

$$\langle \Delta U \rangle = -2.80224 + 3.35077\langle \text{T-O} \rangle - \langle \text{T-O} \rangle^2. \quad (3)$$

The Si- and Al-bonded oxygen atoms are represented by Gaussian distributions with half-widths $\langle \Delta U_{(Si)} \rangle$ and $\langle \Delta U_{(Al)} \rangle$, respectively, located at distances d(Si-O) and d(Al-O) from the tetrahedron center. The distribution that represents both oxygen types is therefore non-Gaussian and its second moment is given in algebraic form by Equation 1. The predicted effect of positional disorder on the oxygen displacement amplitude (and $\langle \Delta U \rangle$) is depen-

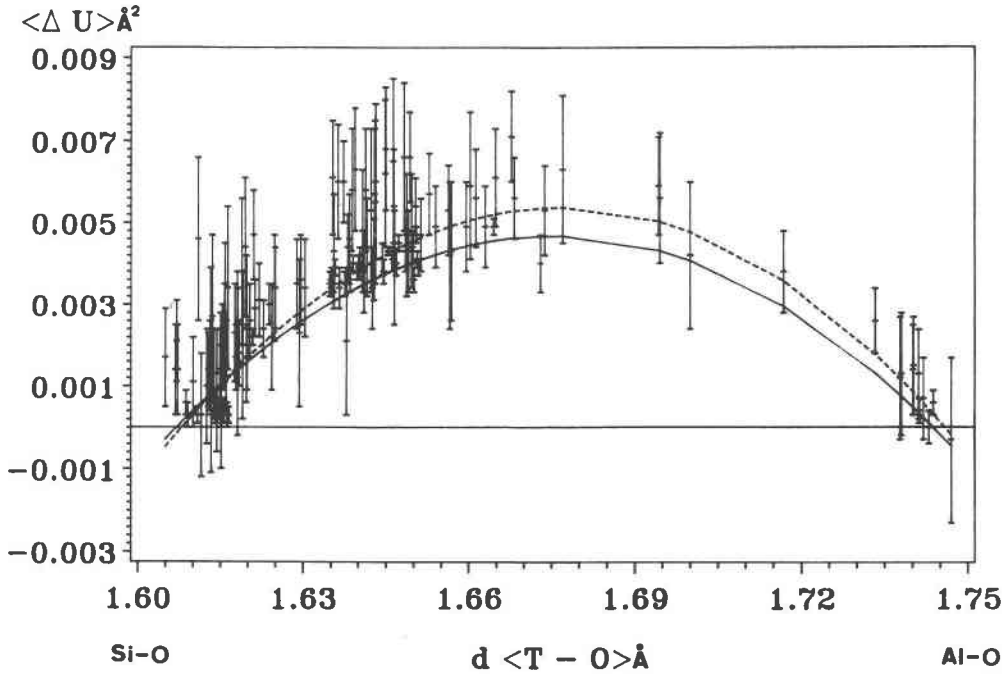

Fig. 3. Variation of $\langle \Delta U \rangle$ (Å^2) with $\langle$T-O$\rangle$ (Å) in alkali feldspar tetrahedra with varying (Si,Al) occupation. 143 tetrahedra from 49 structures are displayed as solid bars representing $\langle 2\sigma(\Delta U) \rangle$. Outliers as discussed in the text have been omitted. The solid curve through the data represents a theoretical model of Eq. 1. The dashed curve results from a weighted ($w = 1/\sigma^2$) quadratic regression.

dent on the population of the two oxygen sites and reaches a maximum for tetrahedral sites statistically occupied by 50% Si and 50% Al.

Discussion

When comparing the calculated function with the observed $\langle \Delta U \rangle$ values in alkali feldspars (Fig. 3), a good general agreement is striking. However there are nine outliers to be explained that are not displayed in Figure 3. β_{22}(T$_2$O) of high albite (Ribbe et al., 1969) is misprinted in the original table. Four outlying tetrahedra (Weitz, 1972) belong to structure refinements of two sanidines from the Eifel district, F.R.G. Several similar sanidines from the Eifel have been examined (Phillips and Ribbe, 1973; Gering, 1985) and fit well into the theoretical model. Unfortunately, there is very little information concerning experimental and refinement procedure, so that the misfit of the Weitz data cannot be explained. Rather high $\langle \Delta U \rangle$ values accompanied by the highest standard deviations in the data set were calculated for a strained intermediate microcline intergrown as untwinned lamellae in a cryptoperthitic ternary feldspar (Ribbe, 1979). The nine outliers were not included in a quadratic regression analysis of the observed values, yielding $\langle \Delta U \rangle = -3.0139(1069) + 3.6063(1279)\langle$T-O$\rangle - 1.0767(382)\langle$T-O$\rangle^2$ with weighting scheme w = unit weight, and $\langle \Delta U \rangle = -3.1728(638) + 3.7905(764)\langle$T-O$\rangle - 1.1302(229)\langle$T-O$\rangle^2$ with $w = 1/\sigma^2$. The refined parameters are in good agreement with the theoretical model in Equation 3. Excellent agreement is even observed between the theoretical model and the precise X-ray and neutron diffraction data on sanidines and orthoclase by Gering (1985). These data also show the lowest esd's in Figure 3.

Conclusions

(1) Difference displacement parameters, $\langle \Delta U \rangle$, evaluated along the T-O vectors in alkali feldspar tetrahedra are largely independent of the temperature of data collection. (2) $\langle \Delta U \rangle = 0.0004$ Å^2 is calculated for an SiO_4 tetrahedron and $\langle \Delta U \rangle = 0.0005$ Å^2 for an AlO_4 tetrahedron. (3) With increasing (Si,Al) disorder, $\langle \Delta U \rangle$ values increase; this is explained by the size difference of a SiO_4 and an AlO_4 tetrahedron for which average coordinates are obtained in a (Si,Al)-disordered structure. (4) The correlation between $\langle$T-O$\rangle$ and $\langle \Delta U \rangle$ can be modeled as two juxtaposed Gaussian distribution functions as proposed by Chandrasekhar and Bürgi (1984). (5) Theoretically predicted $\langle \Delta U \rangle$ values for (Si,Al)-disordered feldspars are in good agreement with the observed values. (6) $\langle \Delta U \rangle$ values are shown to be insensitive to intertetrahedral and intratetrahedral distortions in feldspars. On the other hand, they are very useful for detecting errors in structure refinement models or in lists of anisotropic displacement parameters.

Acknowledgments

This study was supported by the Swiss 'National-Fonds,' which is highly acknowledged. We are indebted to H. B. Bürgi for helpful discussions and valuable advice. W. Hummel kindly provided his Crystal Structure Graphic Package (under development) for representation of displacement param-

eters. The manuscript benefited from the reviews of P. H. Ribbe and R. J. Angel.

References cited

Armbruster, Th., Bürgi, H. B., Kunz, M., Gnos, E., Brönnimann, St., and Lienert, Ch. (1990) Variation of displacement parameters in structure refinements of low albite. American Mineralogist, 75, 135–140.

Bailey, S.W. (1969) Refinement of an intermediate microcline structure. American Mineralogist, 54, 1540–1545.

Blasi, A., De Pol Blasi, C., and Zanazzi, P.F. (1981) Structural study of a complex microperthite from anatexis at Mt. Caval, Argentera Massif, Maritime Alps. Neues Jahrbuch für Mineralogie, Abhandlungen, 142, 71–90.

Blasi, A., Brajkovic, A., De Pol-Blasi, C., Foord, E.E., Martin, R.F., and Zanazzi, P.F. (1984) Structure refinement and genetic aspects of a microcline overgrowth on amazonite from Pikes Peak batholith, Colorado, U.S.A. Bulletin Minéralogie, 107, 411–422.

Bürgi, H.B. (1984) Stereochemical lability in crystalline coordination compounds. Transactions of the American Crystallographic Association, 20, 61–71.

Chandrasekhar, K., and Bürgi, H.B. (1984) Dynamic processes in crystals examined through difference vibrational parameters ΔU: The low-spin–high-spin transition in *Tris*(dithiocarbamato)iron(III) complexes. Acta Crystallographica, B40, 387–397.

Chatfield, C., and Collins, A.J. (1980) Introduction to multivariate analysis. Chapman and Hall, London, New York.

Dal Negro, A., De Pieri, R., Quareni, S., and Taylor, W.H. (1978) The crystal structures of nine K feldspars from the Adamello Massif (northern Italy). Acta Crystallographica, B34, 2699–2707.

Gering, E. (1985) Silizium/Aluminium-Ordnung und Kristallperfektion von Sanidinen. Dissertation, Institut für nukleare Festkörperphysik, Kernforschungszentrum Karlsruhe.

Harlow, E. (1982) The anorthoclase structures: The effects of temperature and composition. American Mineralogist, 67, 975–996.

Harlow, E., and Brown G.E. (1980) Low albite: An X-ray and neutron diffraction study. American Mineralogist, 65, 986–995.

Johnson, C.K. (1976) ORTEP II: A Fortran thermal-ellipsoid plot program for crystal structure illustrations. ORNL-5138, U.S. Department of Commerce, National Technical Information Service.

Jones, J.B. (1968) Al-O and Si-O tetrahedral distances in aluminosilicate framework structures. Acta Crystallographica, B24, 355–358.

Keefer, K.D., and Brown, G.E. (1978) Crystal structures and composition of sanidine and high albite in cryptoperthitic intergrowth. American Mineralogist, 63, 1264–1273.

Kroll, H. (1971) Determination of Al,Si distribution in alkali feldspars from X-ray powder data. Neues Jahrbuch für Mineralogie, Monatshefte, 91–94.

Kuchitsu, K., and Bartell, L.S. (1961) Effects of anharmonicity of molecular vibrations on the diffraction of electrons. II. Interpretation of experimental structural parameters. Journal of Chemical Physics, 35, 1945–1949.

Nelmes, R.J. (1969) Representational surfaces for thermal motion. Acta Crystallographica, A25, 523–526.

Phillips, M.W., and Ribbe, P.H. (1973) The structures of monoclinic potassium-rich feldspars. American Mineralogist, 58, 263–270.

Ribbe, P.H. (1979) The structure of a strained intermediate microcline in cryptoperthitic association with twinned plagioclase. American Mineralogist, 64, 402–408.

——(1983) Chemistry, structure and nomenclature of feldspars. In Mineralogical Society of America Reviews in Mineralogy, 2 (2nd edition), 1–19.

Ribbe, P.H., and Gibbs, G.V. (1969) Statistical analysis and discussion of mean Al/Si-O bond distances and the aluminum content of tetrahedra in feldspars. American Mineralogist, 54, 85–94.

Ribbe, P.H., Megaw, H.D., Taylor, W.H., Ferguson, R.B., and Traill, R.J. (1969) The albite structures. Acta Crystallographica, B25, 1503–1518.

Scambos, A.T., Smyth, J.R., and McCormick, T.C. (1987) Crystal structure of high sanidine from the upper mantle. American Mineralogist, 72, 973–978.

Schomaker, V., and Trueblood, K.N. (1968) On the rigid-body motion of molecules in crystals. Acta Crystallographica, B24, 63–76.

Smith, J.V., Artioli, G., and Kvick, Å. (1986) Low albite, $NaAlSi_3O_8$: Neutron diffraction study of crystal structure at 13 K. American Mineralogist, 71, 727–733.

Trueblood, K.N. (1978) Analysis of molecular motion with allowance for intramolecular torsion. Acta Crystallographica, A34, 950–954.

Viswanathan, K., and Kielhorn, H.M. (1983) Al,Si distribution in a ternary (Ba,K,Na)-feldspar as determined by crystal structure refinement. American Mineralogist, 68, 122–124.

Weitz, G. (1972) Die Struktur des Sanidins bei verschiedenen Ordnungsgraden. Zeitschrift für Kristallographie, 136, 418–426.

Winter, J.K., Ghose, S., and Okamura, F.P. (1977) A high-temperature study of the thermal expansion and the anisotropy of the sodium atom in low albite. American Mineralogist, 62, 921–931.

Winter, J.K., Okamura, F.P., and Ghose, S. (1979) A high-temperature structural study of high albite. American Mineralogist, 64, 409–423.

Manuscript received September 14, 1988
Manuscript accepted September 7, 1989

Appendix 1. Correction for rigid-body translation

As mentioned in the text, a possible displacement of the T atom can lead to varying ΔU values along individual T-O bonds. Averaging the ΔU values over the whole tetrahedron leads to a transposition of the origin of the reference system onto the tetrahedron center. The effect of averaging is shown by comparison of two extreme cases.

In case 1, the tetrahedral extension is assumed ideal:

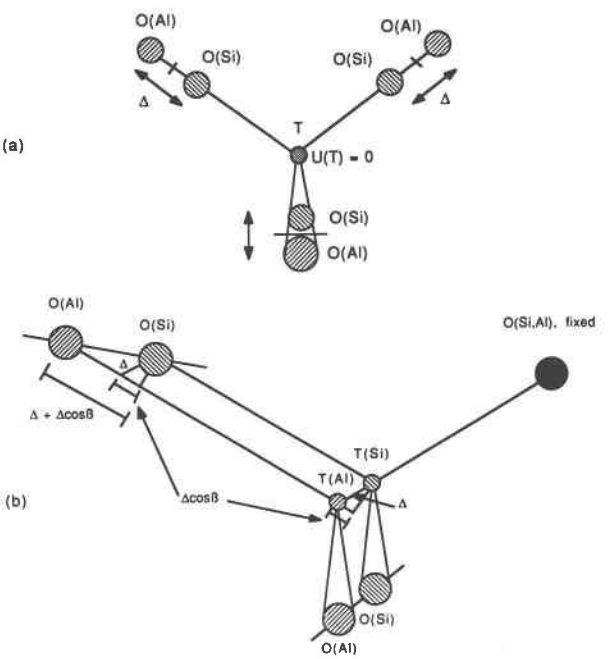

App. Fig. 1. (a) Schematic representation of an ideal tetrahedron, where the T-O extension acts equally on four oxygen atoms. The T atom stays fixed in the center of the tetrahedron. (b) Schematic representation of a tetrahedron, where the T-O extension acts on the T atom and three oxygen atoms, but leaves the fourth oxygen fixed.

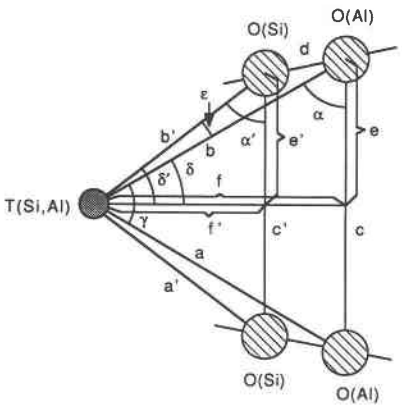

App. Fig. 2. O-T-O section with notations as used for the calculations in App. 2.

Al substitution does not affect the T position in the center of the tetrahedron, but the four oxygen atoms are pushed outward in equal amounts. For illustration and notation, see Appendix Figure 1a. Δ = amplitude of displacement caused by substitution. $U_{(O)}$ = mean-square amplitude of displacement vector. The difference mean-square displacement amplitude along an individual T-O vector, where $\Delta/2$ is the displacement from a mean oxygen position, is defined as

$$\Delta U = U_{(O)} - U_{(T)} = (\Delta^2/4) - 0.$$

Averaging ΔU values over the whole tetrahedron (four individual T-O bonds) yields

$$\langle \Delta U \rangle = \frac{\sum_{i=1}^{4} \Delta U_i}{4} = \frac{\Delta^2}{4}.$$

In case 2, one oxygen atom remains completely fixed, whereas the remaining three oxygen atoms and the T atom are displaced. For illustration and notation, see Appendix Figure 1b and case 1. α = O-T-O angle = 109.47°. β = complementary angle to α; therefore, β = 70.53°.

App. Table 1. Results of principal-component analysis on distances in $(Si,Al)O_4$ tetrahedra (type T_1)

Vector	Mean distance (Å)	Eigenvectors (eigenvalue = 9.58)
T_1-O_A	1.6595(523)	0.986
T_1-O_B	1.6522(505)	0.990
T_1-O_C	1.6612(442)	0.984
T_1-O_D	1.6648(471)	0.986
O_A-O_B	2.6457(578)	0.920
O_A-O_C	2.7657(1119)	0.966
O_A-O_D	2.6530(605)	0.986
O_B-O_C	2.7281(981)	0.992
O_B-O_D	2.7357(827)	0.993
O_C-O_D	2.7077(826)	0.984

Note: Standard deviations in parentheses.

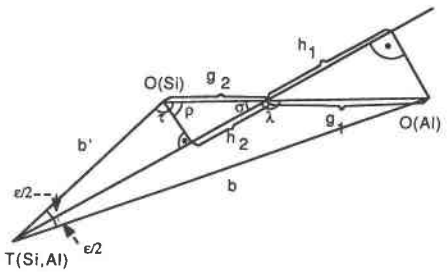

App. Fig. 3. Enlarged T-$O_{(Si)}$-$O_{(Al)}$ section with notations used in App. 2.

Taking the difference displacement parameter for a fixed oxygen and a shifted T atom and adding the difference displacement parameter for the three shifted oxygen atoms will result in the following:

$$\sum_{i=1}^{4} \Delta U_i = 0 - \frac{\Delta^2}{4} + 3\left(\frac{(\Delta + \Delta\cos\beta)^2}{4} - \frac{(\Delta\cos\beta)^2}{4}\right)$$

$$= -(\Delta^2/4) + [3\Delta^2(1 + 2\cos\beta)](1/4).$$

Substituting $\cos\beta = 1/3$,

$$\sum_{i=1}^{4} \Delta U_i = -(\Delta^2/4) + (3 \times \Delta^2 \times 5/3)(1/4) = \Delta^2.$$

Therefore,

$$\langle \Delta U \rangle = \frac{\sum_{i=1}^{4} \Delta U_i}{4} = \frac{\Delta^2}{4}.$$

Cases 1 and 2 yield the same result. Averaging over the whole tetrahedron removes a T atom displacement and relates the origin of the reference system to the T atom.

Appendix 2. Principal-component analysis

With the eigenvectors of the highest factors (App. Table 1), the mutual influence of intratetrahedral distances can be calculated.

Example: Relation between $d_{(T_1\text{-}O_A)}$ and $d_{(T_1\text{-}O_B)}$

A distance shift in $d_{(T_1\text{-}O_A)}$ by $0.986\sigma_{(T_1\text{-}O_A)}$ = 0.986 × 0.0523 = 0.052 Å leads to a change in $d_{(T_1\text{-}O_B)}$ by

App. Table 2. Prototype SiO_4 and AlO_4 tetrahedra derived from principal-component analysis

Vector	SiO_4 distance (Å)	AlO_4 distance (Å)
T_1-O_A	1.599	1.765
T_1-O_B	1.593	1.755
T_1-O_C	1.610 (fixed)	1.750 (fixed)
T_1-O_D	1.610	1.760
O_A-O_B	2.583	2.754
O_A-O_C	2.518	2.989
O_A-O_D	2.583	2.775
O_B-O_C	2.614	2.927
O_B-O_D	2.639	2.881
O_C-O_D	2.608	2.881

$0.990\sigma_{(T_1\text{-}O_B)} = 0.990 \times 0.0505 = 0.050$ Å. This permits calculations of the mutual ratio of the individual T-O and O-O distances within $(Si,Al)O_4$ tetrahedra. On the basis of these results, prototype SiO_4 and AlO_4 end-member tetrahedra are calculated. The results are given in Appendix Table 2 and are used to derive tetrahedral O-T-O angles and shift vectors.

Example: O_A-T_1-O_B

For notation, see Appendix Figure 2. $a = T_1\text{-}O_A(Al)$, $a' = T_1\text{-}O_A(Si)$, $b = T_1\text{-}O_B(Al)$, $b' = T_1\text{-}O_B(Si)$, $c = O_A(Al)\text{-}O_B(Al)$, $c' = O_A(Si)\text{-}O_B(Si)$.

$$\cos\alpha = \frac{b^2 + c^2 - a^2}{2bc} = 0.78113.$$

Therefore, $\alpha = 38.64°$ and $\delta = 90° - \alpha = 51.36°$.

$$\cos\alpha' = \frac{b'^2 + c'^2 - a'^2}{2b'c'} = 0.80854.$$

Therefore, $\alpha' = 36.05°$ and $\delta' = 90° - \alpha' = 53.95°$. Also, $\epsilon = \alpha' - \alpha = 2.59°$.

The real shift d is calculated as follows:

$$d = \sqrt{(e - e')^2 + (f - f')^2}$$
$$e = b \sin\delta = 1.37056 \text{ Å}$$
$$e' = b' \sin\delta' = 1.28826 \text{ Å}$$
$$e - e' = 0.0823 \text{ Å}$$
$$f = b \sin\alpha = 1.09549 \text{ Å}$$
$$f' = b' \sin\alpha = 0.93759 \text{ Å}$$
$$f - f' = 0.15790 \text{ Å}.$$

Therefore, $d = \sqrt{0.03171 \text{ Å}^2} = 0.17806$ Å.

The projection of d on the bisector of ϵ (for notation, see App. Fig. 3) is determined as follows:

$$\tau = \sin^{-1}[(b \sin\epsilon)/d]$$
$$\sigma = 180° - (\epsilon/2) - \tau = 25.13°$$
$$\rho = 90° - \sigma = 64.87°$$
$$\lambda = 180° - \sigma = 154.87°$$

$$g_1 = [b \sin(\epsilon/2)]/\sin\lambda = 0.09333 \text{ Å}$$
$$g_2 = [b'\sin(\epsilon/2)]/\sin\lambda = 0.08475 \text{ Å}$$

$$h_1 = g_1\cos\sigma = 0.08450 \text{ Å}$$
$$h_2 = g_2\cos\sigma = 0.07673 \text{ Å}$$
$$h = h_1 + h_2 = 0.16123 \text{ Å}.$$

Finally, the difference of the projected real shift and the arithmetic shift may be calculated:

$$(b - b') - h = 0.16125 \text{ Å} - 0.16123 \text{ Å} = 0.00002 \text{ Å}.$$

This separation is below the precision of T-O distances, and a corresponding correction can be neglected.